

# Damage detection in bridge structures including environmental effects

Nguyen V.H.<sup>1</sup>, Mahowald J.<sup>1</sup>, Golinval J.-C.<sup>2</sup>, Maas S.<sup>1</sup>,

<sup>1</sup>University of Luxembourg, Faculty of Science, Technology and Communication,  
Rue Coudenhove – Kalergi, 6; L – 1359 Luxembourg

<sup>2</sup>University of Liege, Department of Aerospace and Mechanical Engineering  
1, Chemin des Chevreuils, B 52; B - 4000 Liège 1, Belgium  
email: vietha.nguyen@uni.lu

**ABSTRACT:** Damage identification for two real big bridges in Luxembourg is carried out in this paper. Vibration responses were captured from different types of excitation such as measurable and adjustable harmonic swept sine excitation and hammer impact. Before, different analysis methods were applied to the data measured from these structures showing interesting results. However, some difficulties are faced, especially due to environmental influences (temperature and soil-behaviour variations) overlaid to the structural changes caused by damage. These environmental effects are investigated in detail in this work. First, the modal parameters are identified from the response data by means of Wavelet Transform. In the next step, they are stochastically collected and processed through Principal Component Analysis. Damage index is based on outlier analysis.

**KEY WORDS:** Civil engineering structures; Damage detection; Principal component analysis; Statistics; Eigenfrequency.

## 1 INTRODUCTION

As for mechanical systems, the condition of civil engineering structures such as bridges may be monitored through vibration features identified regularly during their life. Damage detection is often performed by comparison of modal characteristics between current states and an earlier healthy state considered as “reference”. However, detection based on the comparison of modal parameters like natural frequencies, mode shapes etc. is not always obvious, because damage is not the only source that disturbs those parameters. Indeed, environmental factors, i.e. temperature, temperature gradients, soil-behavior variations, traffic etc., show an important influence on modal parameters as well. It was shown through a bridge’s monitoring in HongKong [1] that the normal environmental changes can bring variance error from 0.2% to 1.52% for the first ten eigenfrequencies. Such a high variation may mask the frequency change due to structural damage, which begs the question: how to remove the environmental effects in the damage detection problem.

In face of the last intricate question, several investigations have been carried out on civil engineering structures. Data reduction is often performed from time sequences into modal features. In [2, 3], damage detection was achieved by some derivatives of Principal Component Analysis and factor analysis where numerical data were collected according to a quite large range of temperature. Furthermore experiments in laboratory [4, 5] and on real structures have been examined. In the last decade, the real bridge Z24 in Switzerland was studied in several works [2, 6, 7] with various methods. Damage detection and localization in the I-40 bridge in New Mexico (USA) was also studied in [5, 8]; however, temperature effect was modeled numerically in [5].

The examples considered in this paper are two bridges located in Luxembourg. The first is named “Deutsche Bank” and the second is the Champangshiehl bridge. Before their demolitions, artificial damages were introduced gradually and the bridges were monitored for a short period. Damage

detection performed on these bridges is addressed in previous works [9-12]. In the “Deutsche Bank” bridge, 31% of prestressed tendons were cut but no crack was observed and the eigenfrequency shift from the intact state to increasing damage levels does not show any tendency. In the case of the Champangshiehl bridge, damages were well detected, but close examination of eigenfrequency shifts and damage indexes did not allow to clearly identify the levels of damages. It was suspected that this could be due to the variation of environmental conditions. In this context, the present work seeks to remove environmental effects, namely temperature or soil-abutment from the bridge diagnosis. The method relies on Principal Component Analysis (PCA) of the identified features, which allows to separate the changes due to environmental variations from the changes due to damage sources. Indication of damage level is based on prediction error of the model.

## 2 METHODOLOGY

Regarding to damage detection, many authors consider eigenfrequencies as good features, although they may be very sensitive to temperature variation. Mode-shapes are less influenced by temperature. In [3], it was shown through a numerical example that damage detection including temperature effect is better when high mode-shapes (modes 6-10) rather than mode-shapes at low frequency are considered as features. However, in real-time monitoring of bridges, modes at high frequency are more difficult to identify from vibration measurements. Therefore the features considered in this paper are eigenfrequencies of the bridge. In a first step, eigenfrequencies are identified by applying the Wavelet Transform on the recorded signals. Next, they are analyzed using PCA in order to differentiate the temperature effect from the damage effect in the feature variations.

The present study exploits the technique and Novelty Index proposed in Reference [2], which does not require any

measurement of environmental parameters because they are considered as embedded variables. Their effect can be simply observed from the variation of the identified features. For the sake of conciseness, the method is briefly recalled here.

If a vector of vibration features  $\mathbf{x}_k \in \mathbf{R}^m$  is identified for an instant  $k$ , let us collect the features in a matrix  $\mathbf{X} \in \mathbf{R}^{m \times N}$ :

$$\mathbf{X} = [\mathbf{x}_1 \ \mathbf{x}_2 \ \dots \ \mathbf{x}_k \ \dots \ \mathbf{x}_N], \quad k = 1, \dots, N \quad (1)$$

where  $m$  is the number of features and  $N$  is the number of samplings. If eigenfrequencies are considered as the features,  $m$  is the number of identified modes. PCA provides a linear mapping of data from the original dimension  $m$  to a lower dimension  $p$ :

$$\mathbf{S} = \mathbf{L}\mathbf{X} \quad (2)$$

where  $\mathbf{S} \in \mathbf{R}^{p \times N}$  is the score matrix which characterizes the environmental-factor space and  $\mathbf{L} \in \mathbf{R}^{p \times m}$  is the loading matrix. The dimension  $p$  presents the number of combined environmental factors disturbing vibration features.

In practice, PCA is often performed by singular value decomposition (SVD) of matrix  $\mathbf{X}$ , i.e.

$$\mathbf{X} = \mathbf{U}\mathbf{\Sigma}\mathbf{V}^T \quad (3)$$

where  $\mathbf{U}$  and  $\mathbf{V}$  are orthonormal matrices, the columns of  $\mathbf{U}$  defining the principal components (PCs). The number  $p$  of the most important components is determined by selecting the first  $p$  non-zero singular values in  $\mathbf{\Sigma}$  which have a significant magnitude ("energy"). If noise is negligible, environmental factors often show strong influence. Practically for civil engineering structures, temperature reveals itself as the only important environmental factor; in that case  $p$  is limited to 1. The loading matrix  $\mathbf{L}$  may be constructed by the first  $p$  columns of matrix  $\mathbf{U}$ . A residual error matrix  $\mathbf{E}$  is assessed by comparing the original data and the loss of information in the re-mapping of score data  $\mathbf{S}$  back to the original space:

$$\mathbf{E} = \mathbf{X} - \hat{\mathbf{X}}; \quad \hat{\mathbf{X}} = \mathbf{L}^T \mathbf{L}\mathbf{X} \quad (4)$$

For an instant  $k$ , the Novelty Index ( $NI$ ) is defined following the Mahalanobis norm:

$$NI_k = \sqrt{\mathbf{E}_k^T \mathbf{\Delta}^{-1} \mathbf{E}_k} \quad (5)$$

where  $\mathbf{\Delta} = (\mathbf{X}\mathbf{X}^T)/N$  is the covariance matrix of the features. Let us note  $\overline{NI}_r$  and  $\sigma$  respectively the mean and standard deviation values of  $NI$  in the reference state, an outlier limit may be estimated by the value:  $OL = \overline{NI}_r + 3\sigma$ . A state may be identified as a damage state when a considerable percentage of samples exceed the outlier limit and when the ratio  $\overline{NI}_d/\overline{NI}_r$  is high where  $\overline{NI}_d$  is the mean value for the current state.

### 3 APPLICATIONS

#### 3.1 The "Deutsche Bank" bridge

It is a three-span concrete bridge with a total length of 51m, post-tensioned by 29 tendons with subsequent grouting (Figure 1). In order to simulate damage due to corrosion, several prestressed tendons were cut locally at different positions as pointed out in Table 1. The data considered in this work were achieved after the removal of asphalt layer (170t) that reduced mass rather than stiffness of the structure. Under the excitations of an electric shaker, vibration responses of the bridge were captured by 12 sensors allocated on two sides of

the bridge deck. They are presented by points 115, 127, 135, 210, 215, 227, 235, 240, 245, 255, 260 and 340 in Figure 2.

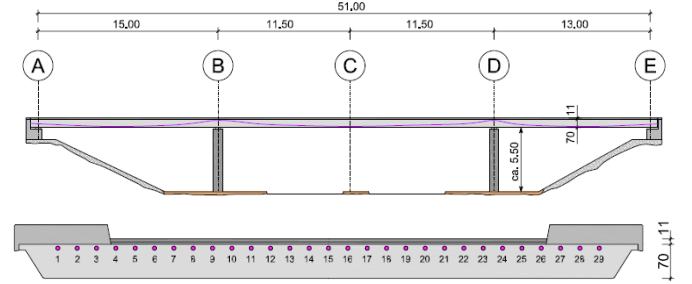


Figure 1. The elevation and the cross-section (axis B/D) of the "Deutsche Bank" bridge

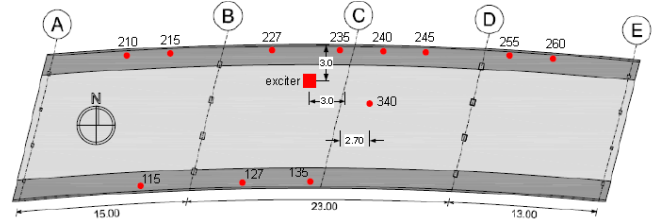


Figure 2. Measurement setup for dynamic tests

Table 1. Description of the damage scenarios according to the cutting sections shown in Figure 1

| State | Description   |
|-------|---|
| # 0   | Intact state  |
| # 1   | Cutting of 1 tendon, n° 15, axis C                            |
| # 2   | Cutting of 5 tendon, n° 7,13,15,17,23, axis C                 |
| # 3   | Cutting of 9 tendon, n° 5,7,9,13,15,17,21,23,25, axis C       |
| # 4   | Cutting of 9 tendon, n° 5,7,9,13,15,17,21,23,25, Axis B, C, D |

Table 2. Eigenfrequencies identified by MEscape

| State | # 0   | # 1   | # 2   | # 3   | # 4   |
|-------|-------|-------|-------|-------|-------|
| $f_1$ | 4.15  | 4.17  | 4.13  | 4.12  | 4.20  |
| $f_2$ | 5.08  | 5.08  | 5.06  | 5.11  | 5.13  |
| $f_3$ | 10.20 | 10.20 | 10.20 | 10.20 | 10.30 |
| $f_4$ | 11.90 | 12.00 | 12.00 | 12.00 | 12.00 |

Because of the safety regulations and time restrictions, no further damage was recorded before the demolition.

As reported in [12], the measurements at the center of the mid-span showed an increase of about 15% in the static vertical displacement and of about 35% in the longitudinal strain of the passive reinforcement all along the damage scenarios. Modal analysis was carried out by means of the Global Polynomial method available in the MEscape software and shown in Table 2 [13]. However, by observing dynamic responses such as eigenfrequencies and damping ratios, no damage could be discovered [12, 13]. It concerns with the cutting of the third of tendons (9 out of 29) that may be inadequate to provoke visible crack. (Due to the removal of the asphalt layer, stresses did not exceed tensile strength of concrete). As for ambient condition, the bridge was tested during 10 days in autumn with no significant weather alterations. However, the environmental variation may mask

changes in modal parameters and so obstruct the detection of the produced damages. But unfortunately, no complete monitoring of temperature was achieved.

In the present work, to exploit statistical Novelty Index cited above, modal parameters are identified here using the Wavelet Transform (WT) and eigenfrequencies are chosen as system features. The reason is that the data obtained by WT responses are abundant, so that each eigenfrequency may be periodically picked up to 600 times for each state. In total there are 3000 sets of results for all the states. They are plotted in Figure 3 for the first four modes.

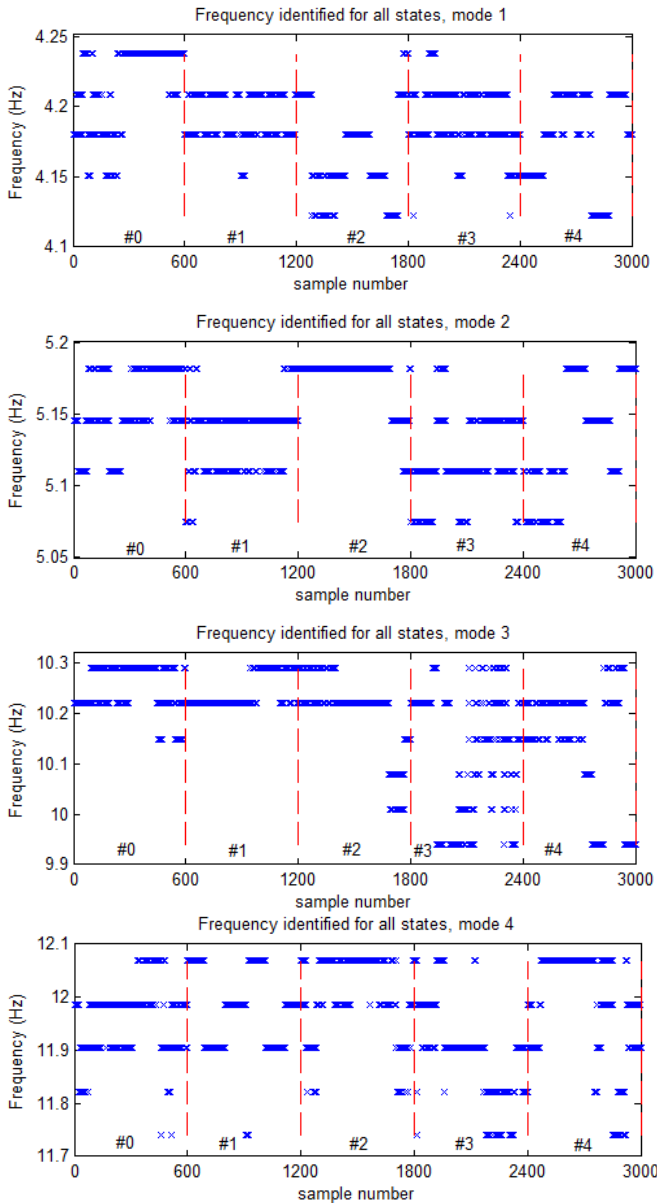


Figure 3. Eigenfrequencies identified for #0 ÷ #4 by Wavelet Transform

Similarly to the results obtained by the Global Polynomial method from Frequency Response Functions in Table 2, the eigenfrequencies identified by the Wavelet Transform (WT) do not reveal any tendency corresponding to the increasing damages. WT frequencies are presented by spectrum and the examined states show different spectrum dispersions. With these dispersions, the observation of eigenfrequencies in

Figure 3 does not give any direct detection of damage. Alternatively, the eigenfrequencies are now collected in the feature matrix  $\mathbf{X}$  according to equation (1) in order to perform PCA detection. To maximize useful information for the PCA procedure, all the four modes are considered. The SVD of  $\mathbf{X}$  (equation 3) for the intact state reveals that the first singular value concentrates about 99% of the energy, which means that only one environmental factor has a significant influence on the four eigenfrequencies. It means that one principal component is enough to characterize the system dynamics. The other singular values are small and may be attributed to the effect of noise; their influence is so small that they do not affect the diagnostics.

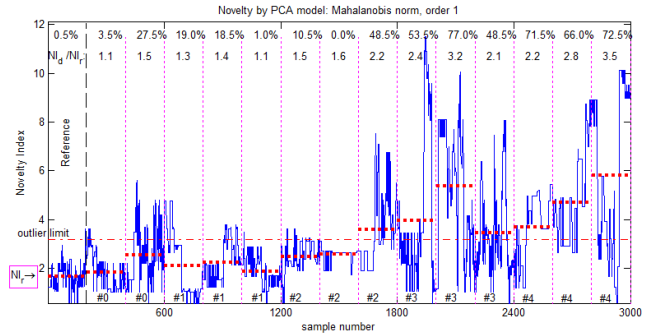


Figure 4. Monitoring of Novelty Index (NI)

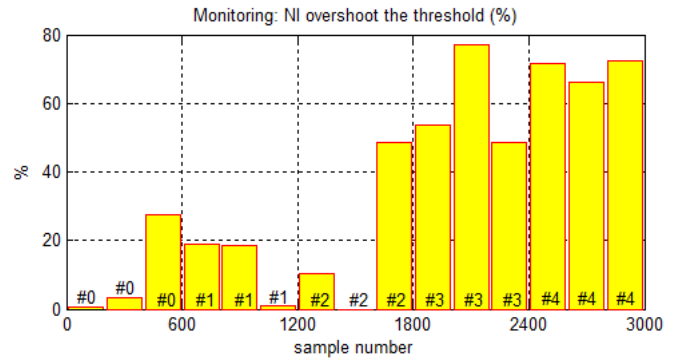


Figure 5. Overshoot rate by NI

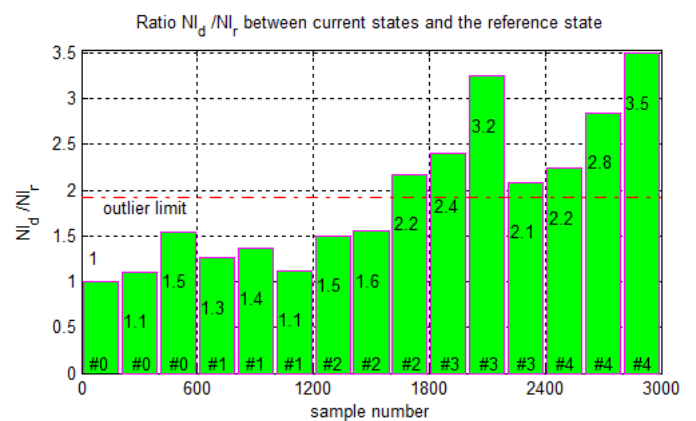


Figure 6. Ratio  $\overline{NI}_d / \overline{NI}_r$

Figure 4 presents the results of the PCA-based detection using the first principal component. In this figure, three data sets are considered for each state. Each data set contains 200 samples. Dotted bold horizontal lines give mean values of the Novelty Index (NI) of all the 15 sets of data. The first healthy set is chosen as reference and its mean value is indicated by  $\overline{NI}_r$ .

The percentage of samples exceeding the outlier limit is given in Figure 5 and the ratio  $\overline{NI}_d/\overline{NI}_r$  in Figure 6. Among the first three set of data including 600 no-damage samples, the third set shows the highest rate of overshoot the outlier limit (27.5%). It relates to the drop of the 3<sup>rd</sup> eigenfrequency (about 10.15Hz) at several samples of that set in Figure 3. However in the whole intact state, this drop is only minority that keeps the mean of  $NI$  always under the outlier limit and the maximum ratio  $\overline{NI}_d/\overline{NI}_r$  is only 1.5. For the first two damaged states #1 and #2, Novelty Index does not show any alarm, except the last set of #2. However, a clear distinction is given from damage #3 when  $NI$  overshoot reaches 50-80%; all  $\overline{NI}_d/\overline{NI}_r$  ratios overpass the outlier limit with values from 2.1 to 3.5. Thus due to small cutting proportion, damages are only detected from state #3, however that is an interesting improvement in relation to former studies in this structure.

### 3.2 The Champangshiehl bridge

With a total length of 102 m, the bridge is divided into two spans of 37 m and 65 m (henceforth noted  $L$ ) respectively (Figure 7). It was pre-stressed by 112 steel wires as illustrated in Figure 8. Before its complete destruction, the bridge was monitored and a series of damages were artificially introduced as summarized in Table 3.

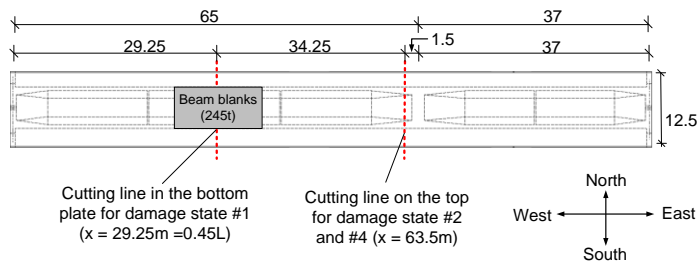


Figure 7. Longitudinal section of the Champangshiehl bridge

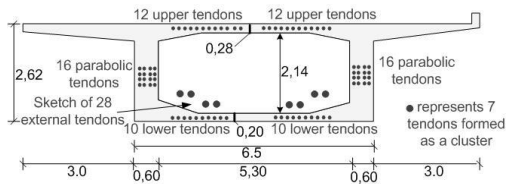


Figure 8. Schematic cross section of the box girder with location of the tendons

The measurement setup considered in the present work is given in Figure 9. Ten sensors were located on each side A and B of the deck (the distance between each sensor is about 10 m). Vibration monitoring under swept sine excitation force and impact excitation were performed on the healthy structure and at each damage state. More detailed descriptions of the bridge can be found in [11].

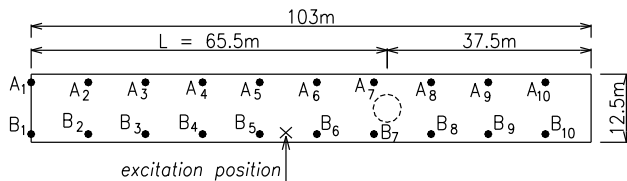


Figure 9. Location of the sensors on the bridge deck

Vibration responses of the bridge in the healthy state and 4 damaged states were recorded during June 2011. Processing of the data was performed in [9, 11] using the Stochastic

Subspace Identification (SSI) method and the Global Polynomial Method. Those earlier analysis can be used for the comparison with the present study combining the Wavelet Transform and the Principal Component Analysis.

Table 3. Description of the damage scenarios according to the cutting sections shown in Figure 8

| State   | # 0             | # 1   | # 2   | # 3                                      | # 4  |
|---|-----------------|---|---|--|--|
| Damage  | Undamaged state | Cutting straight lined tendons in the lower part, at 0.45L (20 tendons) | #1 + Cutting 8 straight lined tendons in the upper part, over the pylon | #2 + Cutting external tendons (56 wires) | #3 + Cutting 16 straight lined tendons in the upper part and 8 parabolic tendons |
| Percentage cutting (100% equals all tendons in the defined) | 0.45L           | 33.7%   | 33.7%   | 46.1%                                    | 46.1%  |
|   | Over the pylon  | 0%  | 12.6%   | 24.2%                                    | 62.12%   |

Moreover, in order to broaden false-positive tests that avoid false alarms for undamaged states, data in the healthy condition are enriched and gathered from different days and different excitations. As presented in Figures 10 and 12, two sections #0 correspond to the impact and then swept sine excitations, respectively, which were performed in two separate days. The damaged states are examined under the swept sine excitations.

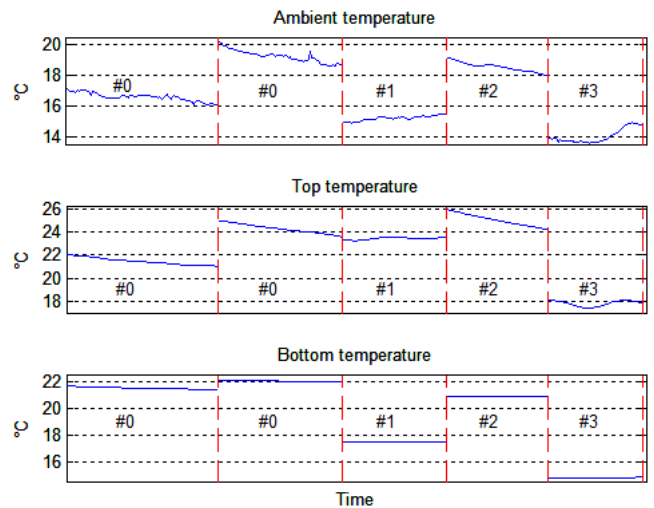


Figure 10. Evolution of the temperature during states #0 ÷ #3 (no data recorded for state #4)

During the monitoring of the bridge, temperature was also measured outside and inside of the bridge. As all the states were carried out one after the other and so recorded at different days in June, the environmental conditions changed from one measurement set to the other. Figure 10 displays the

ambient temperature (under the bottom plate of the superstructure) as well as temperatures measured at the top and at the bottom of the bridge. For security reason, the temperature monitoring system was removed before the most significant damage #4 so that the temperature was not recorded for the last state.

Modal identification and damage detection were performed in [9-11] without taking into account temperature variations. It gave the results shown in Table 4 and Figures 11, 12.

Table 4. Change in the eigenfrequencies (identified by the SSI method)

|                  | #0<br>(H) | #1<br>(D1) | #2<br>(D2) | #3<br>(D3) | #4<br>(D4) |
|------------------|-----------|------------|------------|------------|------------|
| $f_1$ (Hz)       | 1.92      | 1.87       | 1.95       | 1.82       | 1.75       |
| $\Delta f_1$ (%) |           | -2.6       | +1.6       | -5.21      | -8.85      |
| $f_2$ (Hz)       | 5.54      | 5.45       | 5.24       | 5.39       | 5.3        |
| $\Delta f_2$ (%) |           | -1.62      | -5.42      | -2.71      | -4.33      |

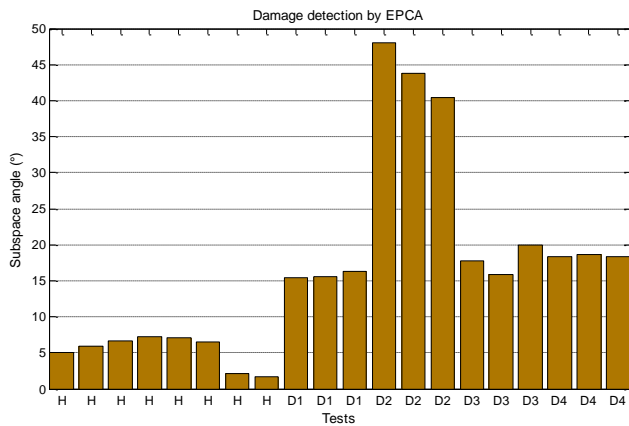


Figure 11. Damage detection by Enhanced PCA [9]

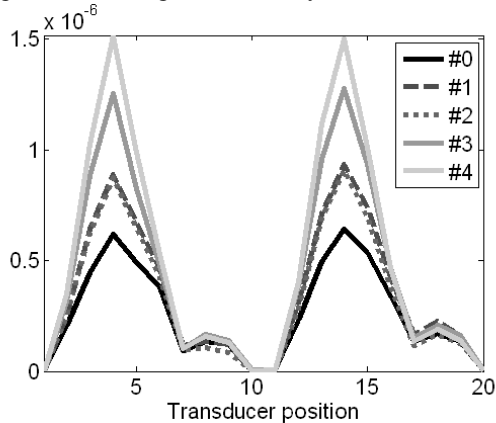


Figure 12. Damage detection based on diagonal elements of the flexibility matrix

It can be asserted from Table 4 and Figures 11-12 that all the damage states are well detected. However, according to these results, state #2 shows a particular behavior: the frequency of mode 1 increases slightly with respect to the healthier states while the frequency of mode 2 exhibits the most important drop. The variation of temperature shown in Figure 10 may be suspected as responsible for this particular behavior. For damaged state #2, the corresponding ambient temperature does not look unusual as it is in the same range of the ambient temperature recorded for the healthy state #0; however the

temperature at the top of the bridge during state #2 is the highest. This observation is probably the reason why state #2 has a non-conventional behavior compared to the other states. In the following, it will be shown that the proposed method allows to answer this problem.

As said before, eigenfrequencies are identified here using the Wavelet Transform (WT) and are chosen as system features. Each eigenfrequency is here periodically picked up to 300 times for each damaged state, and  $2 \times 300$  times for the reference state. In total there are 1800 sets of results for all the states. They are plotted in Figure 13 for the first four modes. The first and the third eigenfrequencies provide a quite clear distinction between different states as the decrease in frequency is monotonous from one state to the others. However, the identification results confirm that the second and fourth eigenfrequencies do not allow to detect damage except in states #3 and #4 for the second mode and only in state #4 for the fourth mode.

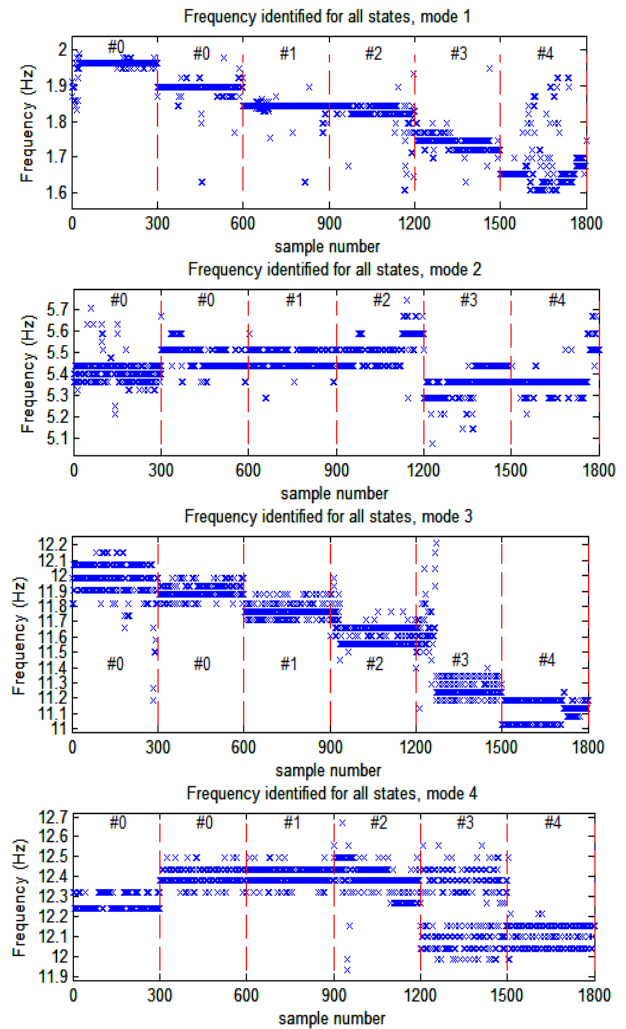


Figure 13. Eigenfrequencies identified by WT for #0 ÷ #4

With the first singular value occupying near 100% of energy, the SVD of vibration feature matrix  $\mathbf{X}$  shows also that there is only one environmental factor which influence the most on the features. In this case, the environmental factor is the temperature (it is the only one that is noticeable). Thus 1 principal component is kept to define the loading matrix to



characterize the environmental-factor space. The PCA detection is shown in Figures 14 and 15 that for each case of damage, three data sets are considered and the reference state has six data sets. Each data set contains 100 samples.

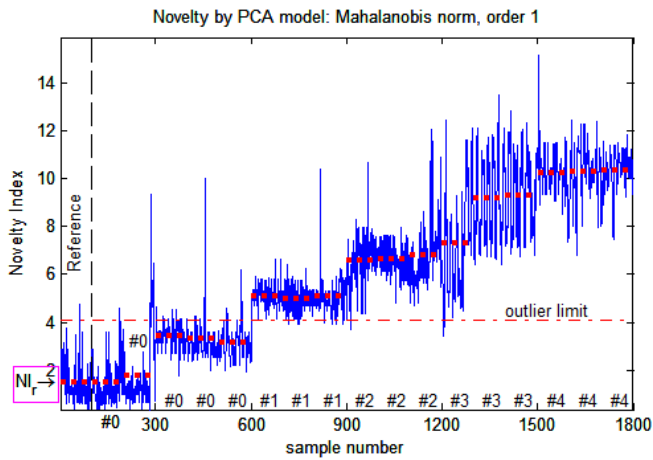


Figure 14. Monitoring of Novelty Index (NI)

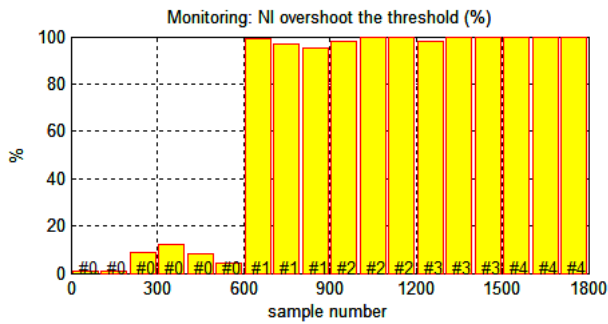


Figure 15. Overshoot rate by NI

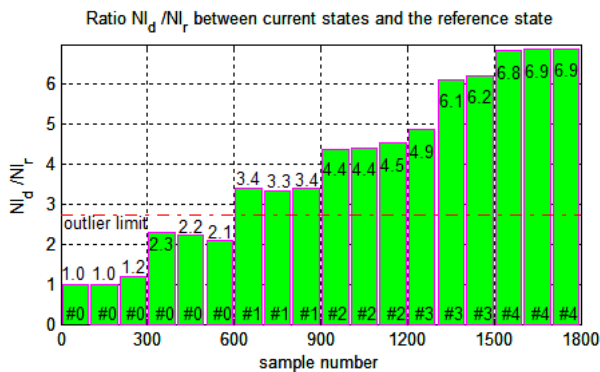


Figure 16. Ratio  $\overline{NI}_d / \overline{NI}_r$

An overall look at Figure 14 reveals an interesting result: despite the variation of the  $NI$  for the 6 undamaged states #0 (which results from the variation of the eigenfrequencies with the temperature), most of the  $NI$  values lies below the outlier limit line. The few samples crossing this line are influenced by other factors (presence of nonlinear effects, noise). Figure 14 also reveals that all the damage states are detected and well classified in accordance with their levels. Despite the fact that all healthy states are not measured continuously and that their temperature range does not cover every states, consistent results are obtained.

In Figure 15, the percentage of  $NI$  overpassing the limit is close to 100% for all the damaged states showing that even the smallest damage is clearly detected. In Figure 16, the ratio

$\overline{NI}_d / \overline{NI}_r$  is use to exhibit the progression of damage. By the distinct levels of damage, each damaged state is clearly classified from undamaged state with homogenous ratios.

#### 4 CONCLUSION

Data recorded from two real concrete bridges are processed in this paper. Sometimes an increase of eigenfrequencies follows a damage of increasing level, which is not theoretically expected. The same phenomenon was observed in other structure like in the bridge I-40 in New Mexico (cited in [5, 8]). Environmental effects that are assumed responsible of this phenomenon could be removed using PCA of the identified features (eigenfrequencies in this work) and statistics as damage indexes. The present work shows meaningful improvements with respect to earlier analyses [9-13]. In previous studies on the “Deutsche bank” bridge, the damages were not directly detected by modal features. As discussed in [12], it may be a consequence of prestressed structures: visible cracks appear very late, shortly before collapse and only with important damage. Non-sizable damage is not revealed directly from the monitoring of modal parameters. In the particular case of the Champangshiehl bridge, damage #2 showed uncommon behaviors (apparent by eigenfrequency, damage index [9]). This uncommon behavior is cancelled out through damage indexes used in this paper. It shows that the detection in the Champangshiehl bridge is clearly easier than in the “Deutsche bank” because the cutting ratio is considerably higher in the Champangshiehl bridge.

As for damage indices, the  $\overline{NI}_d / \overline{NI}_r$  ratio is not in the same range for every structure in healthy state. So looking in the overshoot rate is also an inherent task which may give more accurate information.

The advantage of the detection here is its simplicity. No-environmental measurement is needed. The feature collection is achieved by Wavelet Transform, then PCA is used for analysis, they are all very practical and convenient for automation. It is shown that even if reference data is not collected according to a full range of temperature covering other states, the detection is still faithful.

#### ACKNOWLEDGMENTS

The author V. H. Nguyen is supported by the National Research Fund, Luxembourg.

#### REFERENCES

- [1] J. M. Ko , K. K. Chak , J. Y. Wang, Y. Q. Ni, T. H. T. Chan , *Formulation of an uncertainty model relating modal parameters and environmental factors by using long-term monitoring data*, Smart Structures and Materials 2003: Smart Systems and Nondestructive Evaluation for Civil Infrastructures, 298, 2003.
- [2] A.-M. Yan, G. Kerschen, P. De Boe, J.-C. Golinval, *Structural damage diagnosis under varying environmental conditions- Part I, II*, Mechanical Systems and Signal Processing 19, pp. 847-880, 2005.
- [3] Deraemaeker, Reynders, De Roeck, Kullaa, *Vibration-based structural health monitoring using output-only measurements under changing environment*, Mechanical Systems and Signal Processing 22, pp. 34-56, 2008.
- [4] J. Kullaa, *Elimination of environmental influences from damage-sensitive features in a structural health monitoring system*, Structural Health Monitoring – the Demands and Challenges, CRC Press, in Fu-Kuo Chang (Ed.), Boca Raton, FL, pp. 742-749, 2001.
- [5] M.P. Limongelli, *Frequency response function interpolation for damage detection under changing environment*, Mechanical Systems and Signal Processing 24, pp. 2898-2913, 2010.

- [6] J. Kullaa, *Damage detection of the Z24 bridge using control charts*, Mechanical Systems and Signal Processing 17(1), pp. 163-170, 2003.
- [7] E. Reyders, G. Wursten, G. De Roeck, *Output-only structural health monitoring by vibration measurements under changing weather conditions*, Proceedings of the third International Symposium on Life-Cycle Civil Engineering IALCCE, 3-6 October 2012, Vienna, Austria, 2012.
- [8] V. H. Nguyen, J.-C. Golinval, *Damage localization in Linear-Form Structures Based on Sensitivity Investigation for Principal Component Analysis*, Journal of Sound and Vibration 329, pp. 4550-4566, 2010.
- [9] V.H. Nguyen, C. Rutten, J.-C. Golinval, J. Mahowald, S. Maas & D. Waldmann, *Damage Detection on the Champangshiehl Bridge using Blind Source Separation*, Proceedings of the Third International Symposium on Life-Cycle Civil Engineering, IALCCE'12, pp. 172-176, 2012.
- [10] J. Mahowald, S. Maas, F. Scherbaum, D. Waldmann, A. Zuerbes, *Dynamic damage identification using linear and nonlinear testing methods on a two-span prestressed concrete bridge*, Proceedings of the Third International Symposium on Life-Cycle Civil Engineering, IALCCE'12, pp. 157-164, 2012.
- [11] J. Mahowald, S. Maas, D. Waldmann, A. Zürbes, F. Scherbaum, *Damage Identification and Localisation Using Changes in Modal Parameters for Civil Engineering Structures*, Proceedings of the International Conference on Noise and Vibration Engineering, Leuven, Belgium, pp. 1103–1117, 2012.
- [12] S. Maas, A. Zürbes, D. Waldmann, M. Waltering, V. Bungard, G. De Roeck, *Damage assessment of concrete structures through dynamic testing methods. Part 2: Bridge tests*, Engineering Structures 34, pp. 483–494, 2012.
- [13] M. Waltering, V. Bungard, A. Zuerbes, S. Maas, D. Waldmann, *Non-destructive Damage Assessment Using Non-linear Vibration*, International Modal Analysis Conference, IMAC-XXVI, 2008.